

1. Status of SACLA Construction

In February 2011, the manufacture of all the components for SACLA and the high power conditioning of all the RF components were completed. The beam commissioning started on 21st February, and the spontaneous emission at a wavelength of 0.08 nm was observed with the electron beam energy of 7.8 GeV at the end of March 2011. Thus, this five-year construction project for an 8 GeV XFEL facility was completed successfully in March 2011.

In April, the SASE tuning started and, on 7th June 2011, the first SASE laser amplification was successfully observed at a wavelength of 0.12 nm. By this observation, we confirmed that all the components of SACLA have excellent performance as designed.

2. Status of SACLA Operation

2-1. Beam Commissioning

SACLA accelerator commissioning started in February 2011, and the first SASE-FEL light was successfully obtained in June 2011. Figure 1 shows the measured spectrum and transverse profile of XFEL light together with the spontaneous radiation spectrum. During beam commissioning, a beam diagnostic system and a control system were also tested and improved to enable fine tuning of the machine.

Beam tuning was started from the injector section, where the electron beam is compressed by a factor of 20 by velocity bunching. Considering stability and ease of maintenance, a 500-kV pulsed gun with a thermal cathode is used as an electron source in SACLA. The RF phases of the injector cavities were determined by detecting the phase of the self-induced

electromagnetic fields of the electron bunch. Since the beam current from the thermionic gun is about 1 A, a bunch compression factor of 3000 is necessary to obtain lasing, which is roughly one order higher than that of a photocathode system. After the velocity bunching in the injector, the electron beam is further compressed by a three-stage magnetic bunch compressor (BC1~3). The final peak current, more than 3 kA, was confirmed by a C-band deflector cavity installed downstream of BC3.

After fixing the RF parameters, the transverse envelope of the electron beam was adjusted along the accelerator to match the FODO-like magnet lattice of the undulator section. For beam envelope calculation, a linear accelerator model based on a normalized emittance was developed, which is a method commonly used for analyzing the beam dynamics in a storage ring. Since the measurement of a transverse beam profile after BC3 was found to be difficult owing to the intense coherent OTR, several OTR screens were replaced with YAG screens with a spatial mask to remove the coherent OTR.

The electron beam orbit at the undulator section was aligned by monitoring the overlap of the radiation axes of 18 undulators using a monochromator and a CCD, which were located 90 m downstream from the exit of the undulator.

The pulse energy of XFEL light, which was initially about 30 μ J after the first lasing, was increased to 120 μ J at 0.12 nm in autumn by improving the projected emittance and nonlinear correction in the multi-stage bunch compressor. In December 2011, the CeB₆ cathode of the electron gun was replaced with a new one to prepare for the public user operation starting in March 2012.

2-2. Instrumentation Tuning of the Accelerator

The unique characteristics of the SACLA accelerator include high-gradient acceleration with more than 35 MV/m for a compact machine. High precision and reliability are required for achieving a stable X-ray lasing process. To realize these characteristics, the conditioning by high-power RF sources using 50 MW C-band pulsed klystrons was continued throughout almost the whole year of 2011. We finally achieved an acceleration gradient of more than 35 MV/m, as shown in Fig. 2 [1], which is necessary for achieving an electron beam energy of up to 8.3 GeV. To tune electron beams for a stable lasing, well-calibrated beam monitors were important. Therefore, we calibrated a beam position monitor (BPM) and a differential current transformer (DCT) by using the accelerated electron beams. The

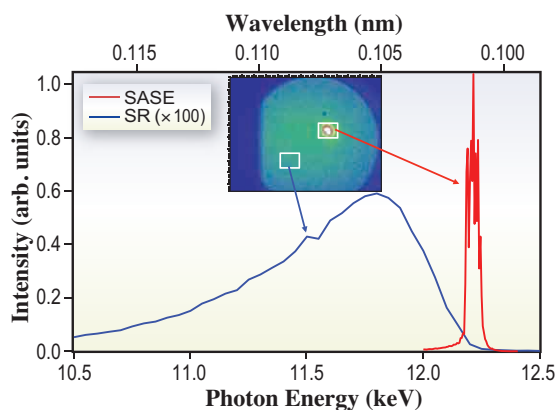


Fig. 1. Measured spectrum of XFEL light (red) and spontaneous radiation (blue). The inset shows the transverse profile of XFEL light.

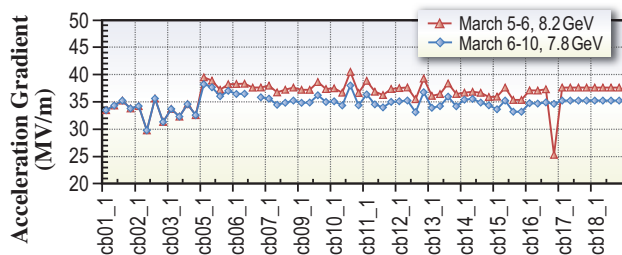


Fig. 2. Acceleration gradient of the C-band accelerator.

calibration data of the BPM and DCT were obtained while changing the beam positions and charges [2,3], as shown in Fig. 3(a) and 3(b). These sensitivities are about $35 \mu\text{m}/0.1 \text{ V}$ and $0.05 \text{ nC}/0.1 \text{ V}$, respectively, which were sufficient for the fine beam tuning of the SACLA accelerator. By using the well-conditioned accelerator, the high-precision beam monitors and the very stable RF system, we realized X-ray lasing with acceptable stability.

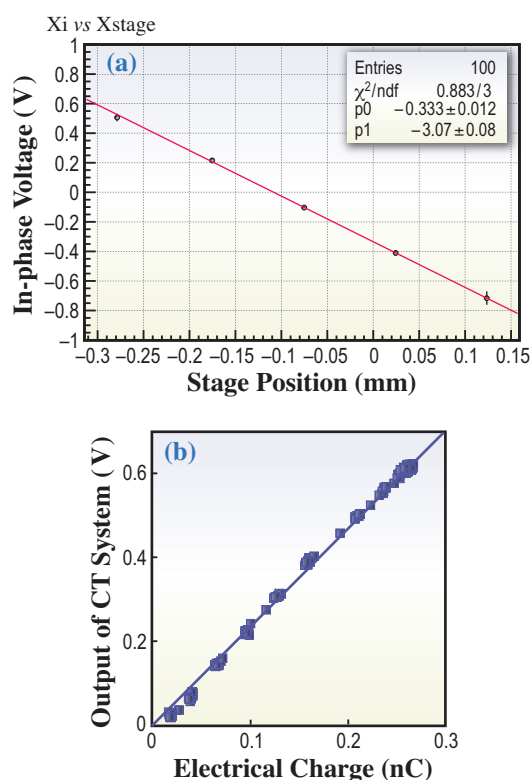


Fig. 3. (a) Calibration of the BPM X-axis. (b) Calibration of DCT charge dependence.

2-3. Undulator Fine Tuning

Undulator fine tuning is a process used to optimize the parameters related to the undulator operation,

which is the final step toward the realization of lasing. We have carried out 5 steps for undulator tuning: fine gap adjustment, undulator height alignment, trajectory correction, phase matching, and undulator taper optimization.

The fine gap adjustment and height alignment are important to ensure that all the undulator segments have the same K value. To carry out these tuning schemes, we measured the spectrum of the spontaneous radiation from a target undulator segment. On the basis of data analysis results together with the theory of undulator radiation, we optimized the undulator gap and adjusted the undulator height. The achieved resolution for each tuning was found to be better than $1 \mu\text{m}$ for the gap and $50 \mu\text{m}$ for the height, which were sufficiently good for achieving FEL saturation.

Next, we attempted the trajectory correction based on the spatial profile measurement of the spontaneous radiation from a target undulator segment. After averaging over 10 shots, we deduced the electron beam angle of injection, which was then corrected by a steering magnet installed just in front of the target segment. The most important feature of this correction scheme is the pointing stability of the electron beam, which has been found to be higher than $1 \mu\text{rad}$, being sufficiently good for satisfying the criterion for trajectory correction.

After the above tuning based on the characterization of spontaneous radiation, we tried two more tuning schemes to enhance the FEL output based on the characterization of SASE radiation. One is the phase matching between undulator segments by tuning the gap of the phase shifter, a magnetic device to create a bump electron orbit in the drift section. The other is the undulator tapering to compensate the energy loss of the electron due to the resistive wake field and FEL interaction. Both optimizations were carried out to maximize the FEL pulse energy measured by the FEL intensity monitor, which is described later.

2-4. Beamline and Experimental Stations

We introduced the first spontaneous radiation ($\lambda = 0.08 \text{ nm}$) into the optics hutch in March 2011. We started precise tuning of the undulator section by using the beamline components in April, and first observed a lasing at a wavelength of 0.12 nm on 7th June. We continued commissioning of the beamline components in the optics hutch and the experimental stations, and performed test experiments with several collaborative research groups.

Figure 4 shows a layout of the beamline in the experimental hall. In the optics hutch, we installed

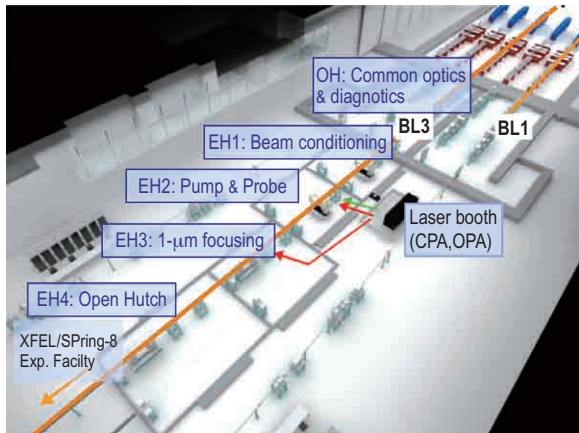


Fig. 4. Beamline layout.

basic optical components (i.e., a double-crystal monochromator (DCM) and a total-reflection mirror system) and key diagnostic devices (i.e., intensity monitors, profile monitors, and a wavelength monitor). We performed precise tuning and calibration of these devices, and confirmed operation as designed.

Figure 5 shows the spatial profile of XFEL light after monochromatization with the DCM, measured 110 m from the exit of the final undulator. We found a stable round-shaped profile with a small angular divergence of $\sim 2 \mu\text{rad}$, which is consistent with a design value. We measured the intensity of XFEL radiation to be $\sim 150 \mu\text{J/pulse}$ at 0.12 nm using a thin-foil intensity monitor [4]. Furthermore, we performed absolute-intensity measurement in collaboration with DESY, PTB, and AIST groups.

For experimental stations, we started commissioning of key devices. In particular, we tuned a focusing mirror

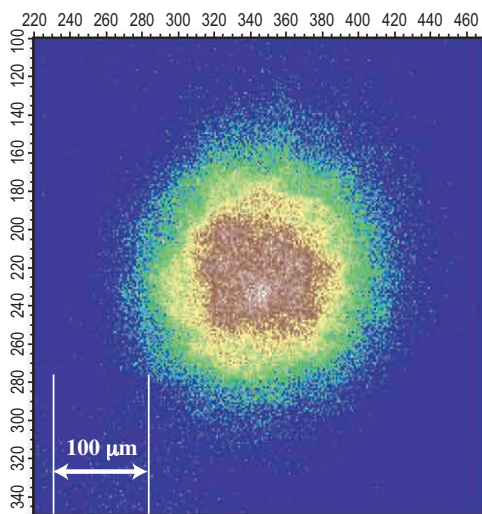


Fig. 5. Spatial profile of XFEL light.

system [5] developed by Osaka University, and obtained a small, intense spot of X-rays with a diameter of $1 \mu\text{m}$. We also performed single-shot measurement of XFEL spectra, and found interesting dependence of the profile on the bunch duration. A preliminary test of the pump-probe scheme combined with an optical laser was performed.

2-5. Detector System

X-ray two-dimensional (2D) detectors optimized for XFEL applications are required to explore the full potential of the XFEL source. As the standard X-ray 2D detector of the SACLA facility, we started to develop a multiport CCD (MPCCD) detector in March 2009. In 2011, two types of MPCCD detector, namely, single- and octal-sensor detectors, were developed. These detectors have been utilized for the commissioning of the accelerator and user experiments. The detector together with a data acquisition system enabled operation stable enough to conduct the user experiments. Advanced 2D sensor development based on silicon-on-insulator sensor technology was carried out. In 2011, the design of a large imaging area of $66 \text{ mm} \times 30 \text{ mm}$ was finalized using the results obtained from a feasibility study of smaller sensor chips. The sensor will provide a higher dynamic range required for the coherent X-ray imaging of samples with sizes of sub-micrometers or larger.

2-6. Control System

The control system was completed on schedule. After the completion of the accelerator control, we modified the system to achieve a higher stability in the summer of 2011. For high power RF and vacuum systems, we increased the number of CPUs to ease the CPU heavy load. Because of the severe timing control of the magnet system, we replaced a VME CPU board with Intel Corei7 and used a busy wait mode for a precise timing. The beamline control system was built on the basis of the “standardization concept” for quick start up. We installed three VME systems for the BL3 control. One was used for the front-end components and transport channel, and the others for the beamline interlock system. As a beamline operation console, SuSE Linux Enterprise 11 with a Xen virtual machine was adopted.

A data acquisition system for the experiments was constructed to handle the 2D X-ray detector (MPCCD), commercial cameras and waveform digitizers, and beamline apparatus in the hutches. The data can be recorded shot-by-shot in

synchronization with X-ray pulses up to 60 Hz. All the data have beam tag numbers as record labels. The data flow up to 5 Gbps from the ten MPCCD sensors has been transferred by the 10 GbE transfer backbone and stored in a high-speed storage since October 2011.

The installation of the interlock systems for the accelerator, BL3, and BL1 was completed in February 2011. An electron beam that deviates from the nominal route may generate unwanted radiations. Therefore, we integrated the beam route monitor and a fast signal transmission system to stop the electron gun. We separated the interlock system into the personnel safety and the machine protection units for sake of simplicity. We developed the interlock status monitoring system by using the FL net that records the operation history onto the database.

3. Operation Status of the SCSS Test Accelerator

At the SCSS test accelerator, research using intense extreme ultraviolet (EUV) light is carried out in a wide variety of disciplines, including technical research in preparation for XFEL experiments, atomic and molecular physics, coherent diffraction imaging methods, studies of damage of optics, materials science such as advanced scintillators, and nonlinear X-ray devices. Fourteen papers were published in 2011 [6-19].

Here, we introduce a result reported by a group led by Professor A. Hishikawa [6]. They observed a new nonlinear photoabsorption pathway in the EUV region involving the joint excitation of two electrons by shot-by-shot photoelectron spectroscopy. They found that the nonlinear process is the three-photon

double excitation of He in the intense EUV-FEL fields, and showed that three-photon double excitation is enhanced by intermediate Rydberg states below the first ionization threshold, giving a greater contribution to the total photoionization yield than the two-photon process by more than 1 order of magnitude. Another result is described in Research Frontiers 2011, page 80 and Ref. [9].

References

- [1] T. Inagaki *et al.*: Proc. IPAC11 (2011) 104.
- [2] H. Maesaka *et al.*: Proc. FEL11, THPA29 (2011).
- [3] S. Matsubara *et al.*: Proc. IPAC11 (2011) 1227.
- [4] K. Tono *et al.*: Rev. Sci. Instrum. **82** (2011) 023108.
- [5] H. Mimura *et al.*: Rev. Sci. Instrum. **79** (2008) 083104.
- [6] A. Hishikawa *et al.*: Phys. Rev. Lett. **107** (2011) 243003.
- [7] E. V. Gryzlova *et al.*: Phys. Rev. A **84** (2011) 063405.
- [8] T. Sako *et al.*: Phys. Rev. A **84** (2011) 053419.
- [9] M. Nagasono *et al.*: Phys. Rev. Lett. **107** (2011) 193603.
- [10] R. Moshhammer *et al.*: Opt. Express **19** (2011) 21698.
- [11] H. Ohashi *et al.*: Nucl. Instrum. and Meth. Phys. Res. A **649** (2011) 163.
- [12] T. Sato *et al.*: J. Phys. B : At. Mol. Opt. Phys. **44** (2011) 161001.
- [13] N.A. Inogamov *et al.*: J. Opt. Technol. **78** (2011) 473.
- [14] R. Bachelard *et al.*: Phys. Rev. Lett. **106** (2011) 234801.
- [15] N.A. Inogamov *et al.*: Contrib. Plasma Phys. **51** (2011) 419.
- [16] T. Shimizu *et al.*: Appl. Phys. Express **4** (2011) 062701.
- [17] M. Yao *et al.*: Eur. Phys. J. Special Topics **196** (2011) 175.
- [18] N. Miyauchi *et al.*: J. Phys. B: At. Mol. Opt. Phys. **44** (2011) 071001.
- [19] T. Togashi *et al.*: Opt. Express **19** (2011) 317.